THE JOURNAL OF PHYSICAL CHEMISTRY B

Article

pubs.acs.org/JPCB

Influence of Ion Size and Charge on Osmosis

James Cannon,*[,†] Daejoong Kim,[‡] Shigeo Maruyama,[†] and Junichiro Shiomi*[,†]

[†]Department of Mechanical Engineering, The University of Tokyo, 7-3-1 Hongo, Bunkyo-ku, Tokyo 113-8656, Japan

[‡]Department of Mechanical Engineering, Sogang University, 505 Adam Schall Hall, 1 Shinsu-dong, Mapo-gu, Seoul, 121-742, Republic of Korea

ABSTRACT: Osmosis is fundamental to many processes, such as in the function of biological cells and in industrial desalination to obtain clean drinking water. The choice of solute in industrial applications of osmosis is highly important in maximizing efficiency and minimizing costs. The macroscale process of osmosis originates from the nanoscale properties of the solvent, and therefore an understanding of the mechanisms of how these properties determine osmotic strength can be highly useful. For this reason, we have undertaken molecular dynamics simulations to systematically study the influence of ion size and charge on the strength of osmosis of water through carbon nanotube membranes. Our results show that strong osmosis occurs under optimum conditions of ion placement near the region of high water density near the membrane wall and of maintenance of a strong water hydration shell around the ions. The results in turn allow greater insight into the origin of the strong osmotic strength of real ions such as NaCl. Finally, in terms of practical simulation, we highlight the importance of avoiding size effects that can occur if the simulation cell is too small.

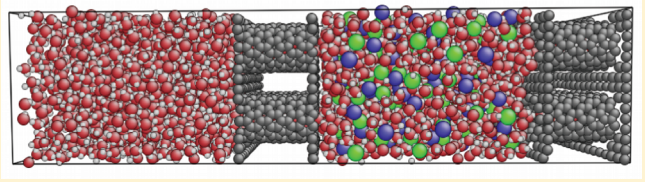

INTRODUCTION

Osmosis is a fundamental process in a wide range of biological and industrial processes. For example, osmosis is the mechanism by which cells in plants, animals, and humans maintain their volume.[1] The impact of osmosis on life can also be indirect whether, for example, in terms of factory processes[2] or in membrane-based desalination methods for clean drinking water.[3,4]

Given the prevalence of osmosis in such a wide range of key processes, it is important to have a detailed understanding of the phenomenon, so that industrial processes can be optimized and so that biological functions be better understood. This is particularly the case for applications such as desalination, where membrane-based reverse-osmosis methods have recently overtaken thermal techniques in popularity,[4] and there is a growing interest in forward osmosis methods which require a strong osmotic pressure gradient.

Although the effect of osmosis can be observed on the macroscale, the process originates through interactions between molecules, and therefore, nanoscale simulation can offer detailed insight into the fundamentals of this process. For this reason, several simulation studies have explored this phenomenon. For example, Kalra et al.[5] studied osmosis through a membrane made of carbon nanotubes by way of molecular dynamics (MD) simulation. Nanotubes are a particularly promising form of membrane for osmotic applications because of their relatively smooth inner structure and because of the potential flow rates that are higher than what conventional theory would predict.[6−10] Corry[11] also used MD simulation to demonstrate the potential effectiveness of nanotubes in achieving significant osmosis for application in desalination technologies, and more recently Jia et al.[9] demonstrated that the strong selectivity of nanotubes coupled with high flow rates may make them ideal for forward-osmosis applications. Beyond studies of nanotube membranes, the MD simulation method is effective and accurate in reproducing osmosis across a range of membranes, whether for very simple fundamental systems[12,13] or for complex reproductions of existing membranes.[14,15]

Central to the process of osmosis is the solute itself. The type of solute dictates the rate of osmosis, and therefore, in industrial applications it is a crucial element in achieving high efficiency. Raghunathan and Aluru,[16] for example, found that the rate of osmosis using NaCl as the draw solute is different from when KCl is used, and they suggested that this was because of the differing affinities of the ions to the membrane as well as the hydration of the ions. It remains unclear, however, to what extent the different atomic properties such as size and charge influence the osmosis and how the inter-relation of ion and water positioning affects the osmosis. This is important when considering what the ideal solute might be for a given application.

We have, therefore, undertaken a systematic simulation study to gauge the effect of solute size and charge on osmotic strength. By making this study, it is our intention to give a greater understanding of what solute qualities affect osmotic strength and to help guide decisions about draw solutes to increase the efficiency of osmosis-based processes and applications.

Received: November 24, 2011
Revised: February 6, 2012
Published: March 8, 2012

dx.doi.org/10.1021/jp2113363 | J. Phys. Chem. B 2012, 116, 4206−4211

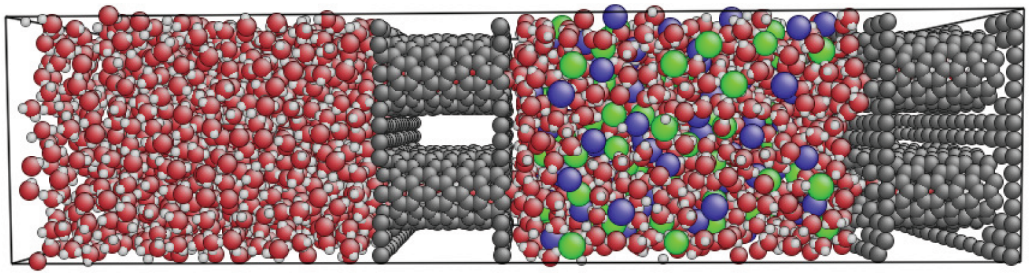

Figure 1. A representative snapshot of the simulation system.

SIMULATION DESIGN

The system design is shown in Figure 1. The left chamber contains pure water (PW), while the right chamber consists of a salt-water (SW) solution. These are separated by a square 2 × 2 array carbon nanotube membrane (four nanotubes in each membrane, eight nanotubes total in the system) with each nanotube of chirality (11,0) and diameter 8.6 Å. The nanotubes have a length of 15 Å, while the length of each chamber is around 45 Å. The lateral x and y dimensions are 30 Å each. Periodic boundary conditions are employed so that the nanotube membranes are essentially infinite, while water is able to flow both left and right between the chambers. A cutoff of 10 Å is utilized for short-range Lennard-Jones (LJ) interactions, while particle-particle particle-mesh (PPPM)[17] methods are used to treat the long-range Coulomb forces. The choice of cutoff distance is a consequence of the 30 Å lateral dimensions of the simulation system taking into account the finite size of the water molecules as well as the balancing of computational accuracy and efficiency.

The open-source software LAMMPS[18] is used for running all the MD simulations in this study. Initially, the system is equilibrated for 4 ns. During this time, through the process of osmosis, some water flows from the pure-water chamber on the left to the salt-water chamber on the right. This causes a decrease in the hydrostatic pressure in the pure-water chamber and a corresponding increase in the salt-water chamber. Despite allowing the pressure in each individual chamber to vary in this manner, to maintain comparability between simulations, the net pressure is maintained constant. This can be understood through eq 1 when denoting the hydrostatic pressure experienced on the left and right walls of the PW chamber as P_{W1} and P_{W2}, respectively, and that on the walls of the SW chamber as P_{W3} and P_{W4} in the same respect.

$$\frac{P_{W1} + P_{W2}}{2} + \frac{P_{W3} + P_{W4}}{2} = K_P \quad (1)$$

The way that this net constant pressure is maintained during equilibration across all simulations is to vary the length of each chamber. Even when accounting for the full range of ion radii considered in this study, the chamber lengths do not change more than 5 Å from the initial 45 Å length. The lengths of the PW and SW chambers are varied in tandem and therefore are equal at all times. It is in principle possible to define the constant K_P in eq 1 in terms of average pressure on the walls of each chamber or in terms of the average force on the walls, K_F, which can then be converted to K_P if required by dividing by the available wall area. We choose to use the latter definition, K_F, because the wall force is directly measurable within MD simulation and because there are inherent difficulties in defining surface area and local pressure at such small scales and in such confined geometries. The value of the constant force K_F is set to be 5.43 nN which corresponds to a prescribed density of 1055 kg/m^3 in each chamber.

The choice of force constant K_F, or its equivalent in terms of pressure K_P, is a result of the desire for the prescribed high density in each chamber in order to force water into the nanotubes. This density does not vary significantly throughout the simulations because the number of water molecules required to flow between the chambers, in order to establish a hydrostatic-pressure osmotic-pressure equilibrium, is relatively small in this small system. Although this density suggests a relatively high pressure, our tests show that it represents one of the minimum densities (i.e., minimum pressures) required for entry of water into carbon nanotubes of this diameter.

This high-density/pressure approach is common in such MD salt-water studies which consider such small nanotubes because it is necessary to generate flow through the nanotubes.[11,19] For example, Raghunathan and Aluru[16] have an initial water density of around 1200 kg/m^3 in their lower-concentration chamber (in addition to 0.3 M of salt) which, considering the relative incompressibility of water, will induce a significantly higher pressure than the one used here. Interestingly, the measured pressure in the study of Raghunathan and Aluru is only 40 bar in each chamber, which would normally correspond to much lower densities of (pure) water, and this highlights the difficulties of defining pressure on the nanoscale. Nevertheless, it is notable that such a density is required to induce flow through these small nanotubes with the implications that this carries for applications making use of such nanotubes.

As the system equilibrates, the hydrostatic pressure across the membranes will grow to oppose the osmotic pressure until the two are in balance. Following this equilibration, the walls are fixed in their final settled position, and the strength of this wall-force difference between the two chambers is measured in order to give an indication of the osmotic strength. Because of the relatively small size, the system is sensitive to thermal fluctuations, and therefore to ensure accuracy, long measurements over 32 ns are performed for each ion radius studied. A time-step of 2 fs is utilized during all simulations resulting in 16 million steps per simulation. This time-step is found to be sufficiently small to maintain good energy conservation throughout the long simulations while minimizing the computational time required.

The salt-water chamber is set at 5 M concentration since it generates sufficiently strong osmosis overcoming thermal noise to allow accurate pressure measurement within reasonable computational time. Although this is much higher than is found, for example, in sea water, comparison to much lower concentrations shows little change in ion hydration, and so the mechanisms and subsequent results will be applicable to lower concentrations too.

dx.doi.org/10.1021/jp2113363 | J. Phys. Chem. B 2012, 116, 4206−4211

Interactions between atoms are governed by Lennard-Jones (LJ) interactions (eq 2) or by coulomb charge interactions. Carbon parameters are derived from water interaction with graphite[20] both for the rigid carbon nanotubes and for the simple membrane wall. For all cross-species interactions, the Lorentz–Berthelot rules[21] are applied. The Extended Simple Point Charge (SPC/E) model[22] is meanwhile used to represent water. The parameters for the salt are based upon sodium (Na) and chlorine (Cl);[23,24] however, to isolate and systematically examine the effect of changing solute radius, hypothetical ions with properties modified from standard NaCl are used. Because ε is the same for both ions, this remains at 0.4184 kJ/mol throughout the study. The mass for each ion is meanwhile set to 30 amu, which is roughly halfway between that of Na and Cl. Variation of the size of the ions is achieved by altering σ, while Na and Cl usually have different values of σ, here $\sigma = \sigma_{Na} = \sigma_{Cl}$ unless stated otherwise, to isolate the effects of specific ion radii. Therefore, unless otherwise stated, for any given simulation, the only difference between the two ion species is that the Na is positive and the Cl is negative. The magnitude of the charge for any given radius remains unchanged from the original value for real NaCl of $\pm 1e$.

$$V(r) = 4\varepsilon\left[\left(\frac{\sigma}{r}\right)^{12} - \left(\frac{\sigma}{r}\right)^{6}\right] \quad (2)$$

SOLUTE SIZE

To have a reference for the osmotic strength of the system, the osmosis-induced pressure difference between the chambers, dP_{real}, is calculated for the case of real NaCl (σ_{Na} = 2.583 Å, σ_{Cl} = 4.401 Å, $\varepsilon_{Na} = \varepsilon_{Cl}$ = 0.4184 kJ/mol,[23,24] where the ions also have their normal mass and charge). Then, when measuring the pressure difference between the chambers for the hypothetical radius-controlled ions, the relative pressure difference dP_{rel} can be calculated in the fashion $dP_{rel} = dP_{this\_radius}/dP_{real}$ where $dP = P_{SW} - P_{PW}$. By using relative values, pressure can be discussed without concern over the accuracy of force-pressure conversion. The value of dP_{rel} for ion radii between 2 Å and 5 Å is shown in Figure 2. Radii above 5 Å were also tested, but in these cases, ions concentrated significantly at the membrane walls resulting in increasing water–ion separation, and it was impossible to obtain a reliable measurement of the pressure difference. This phenomenon of separation is discussed in more detail in the following paragraphs.

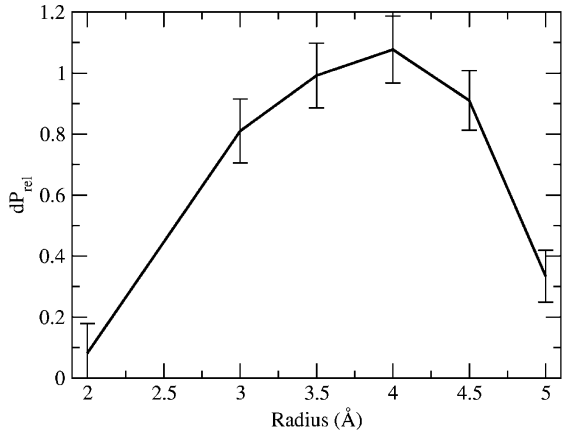

Figure 2. Relative variation of osmotic pressure with ion radius. The error bars indicate one standard deviation.

Figure 2 shows clearly that the medium radii, centered about 3.5–4 Å, induce the strongest osmosis, while that at 2 Å and 5 Å is remarkably weak. To examine the reasons behind this, it is instructive to consider the interaction of the ions with water (Figure 3). The graph shows that as the solute radius increases,

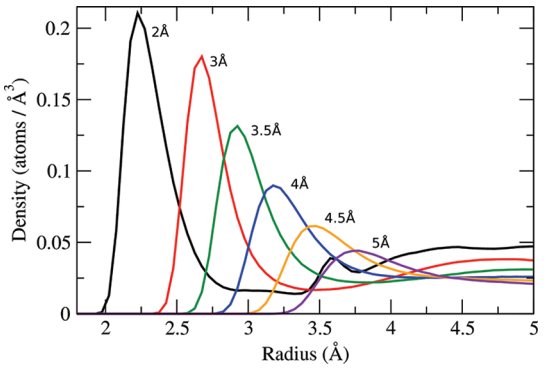

Figure 3. Variation in radial density of water around the Na ion in the salt-water chamber for different ion radii. The peak density of water is seen to decrease as the ion radius increases. A similar variation is observed for the Cl ion.

the peak density of water around the ions decreases. This is intuitive, since as the water is able to approach more closely to the ions, the coulomb interaction becomes stronger and therefore water is more tightly (and more densely) bound. Because osmosis occurs on the basis of this coulomb attraction of water to ions, the strongest osmosis would also be expected to occur for the smallest ions which pull on the water most strongly; however, this has been observed not to be the case. As the following paragraphs explain, this is because the hydration of the ions not only affects their interaction strength but also their position in the SW chamber.

As the binding of water to the ions becomes weaker with increasing ion radius, the ions can be observed to be increasingly positioned toward the membrane wall (Figure 4). This can be understood in two ways. First, for the ions to approach the membrane wall, it is necessary to reduce the number of water molecules in the hydration shell between the ion and the wall, and this is easiest to do with the largest ions

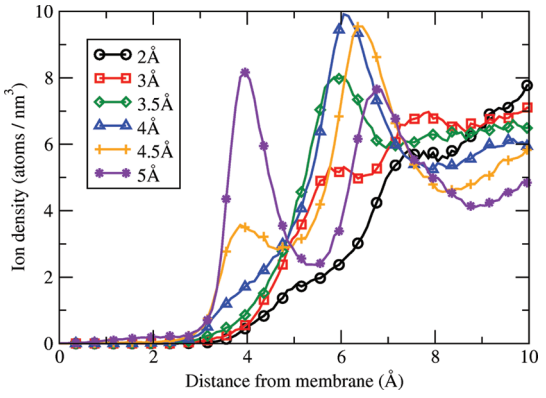

Figure 4. Variation of ion density (Na + Cl) with distance from the nanotube membrane. As the solute size increases, the density near the membrane also increases. Values are an average from the left and right walls of the SW chamber.

dx.doi.org/10.1021/jp2113363 | J. Phys. Chem. B 2012, 116, 4206–4211

because of the relatively weak binding between the two (the size of the hydration shell is more important for the positioning of the ion than any effect induced by the size of the ion itself). The smaller ions are seen to be held at a distance from the membrane that is consistent with the existence of their strongly bound hydration shell, while the largest ions display a two-peak density formation consistent with reduced hydration and the tentative emergence of layering at the membrane. Second, the larger the ion, the less hydrophilic it effectively is as the strength of the coulomb interaction with water drops leading to increasing ion−water separation. For radii greater than 5 Å, this results in very high concentration of ions at the wall making it impossible to accurately measure the pressure. The water is correspondingly separated from these large ions situated toward the center of the chamber.

The 2 Å ion system also experiences water−ion separation to some extent; however, in contrast to the large radii where it was the weakening water−ion interaction that led to the separation, here it is the increasing ion−ion interaction which is driving the separation. This causes an asymmetry in the distribution of the ions in the SW chamber as the ions begin to move as a group and are weakly attracted to one of the two membrane walls at random. Thus, the osmosis between 2 Å and 5 Å can be seen in the context of a transition between the two extremes of more-hydrophilic and more-hydrophobic ions. Indeed, in the extreme case where the charge on the ions is simply turned off, the ions are forced into the nanotubes while the water forms an energetically favorable structure in the center of each chamber. The bare ions are small enough to enter the nanotubes, and it is only the binding of the water in the form of a hydration shell which increases their effective size and which prevents them from entering.

For the ions to induce an osmotic pressure, they need to pull water into the SW chamber by attracting water through coulomb interaction. One can expect that this is most effectively performed when this attractive force is concentrated near the membrane itself because movement of water from a location near the membrane deeper into the SW chamber is more encouraging of osmotic flow compared to the movement of water already situated deep inside the chamber. Furthermore, any short-lived hydrogen bonds may enhance osmosis by transferring the movement of water near the membrane onto water further back or even inside the nanotubes themselves.

Figure 5 shows how, as a consequence of their position, the application of force by the smallest ions is concentrated further from the membrane wall compared to other ions. This means that despite the strong interaction with water, the contribution to osmosis is relatively ineffective resulting in the low osmotic pressure observed. In contrast, while the largest ions do have their peak application of force near the membrane wall, this force is relatively weak. This arises for two reasons: first, their weak hydration results in weak pull on the water, and second, the very close positioning of the ions to the wall is not optimum for pulling water toward the center of the chamber particularly at the peak water density at 3 Å. The strong osmosis experienced by the medium radii can therefore be understood as a result of optimum positioning of ions for application of force on water near the membrane wall (particularly on water at the 3 Å peak density) while still maintaining relatively strong hydration.

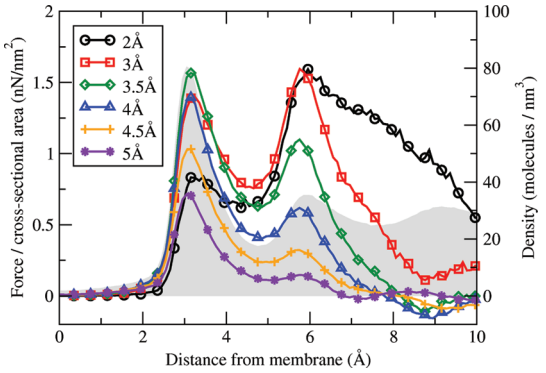

Figure 5. Lines: Coulomb force by ions on water per cross-sectional area. Shaded area: Density of water. Because of the relative densities of the ions and water, the greatest application of osmotic pull by the ions occurs at 3 Å and, to a lesser extent, at 6 Å.

RELATION OF SOLUTE SIZE TO CHARGE AND THE INFLUENCE ON OSMOSIS

Having observed the influence of solute size on osmosis, it is interesting to consider another key variable that describes the properties of salts: the charge. For real-world osmotic applications, the drawing solution can utilize ions with single charge such as NaCl or indeed double charge such as Mg_2 + Cl_2,[25] and it is interesting to consider coupling between optimum charge and optimum solute radius because both influence the hydration of the ions and their subsequent position.

To investigate this, the ions radius of 4 Å is considered, and the magnitude of the charge on the ions is varied. In each case, the magnitude of the charge on the positive and negative ions is the same. Figure 6 shows the transition in the strength of the osmosis with charge. For charges of 0.6e, the ions lose enough of their hydration shell that they are able to pass to the PW chamber leading to a breakdown in the osmotic process. It was noted earlier how ions with no charge fill the nanotubes at the expense of the water, which is in contrast to the lightly charged ions passing through to the PW chamber. Therefore, the mechanism of breakdown of osmosis for lightly charged and no-charge ions is somewhat different even while the result (i.e., no osmosis) is the same.

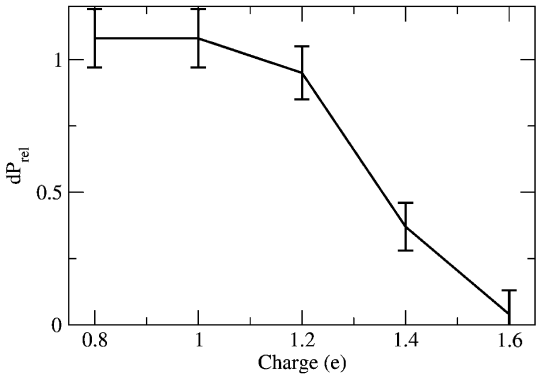

Figure 6. Relative osmotic pressure induced for the 4 Å ion system as a function of charge on the ions. The 0.6e charge was found to leak ions from the SW chamber to the PW chamber preventing osmosis. Charge around 1e can be seen to be optimum for this 4 Å case.

dx.doi.org/10.1021/jp2113363 | J. Phys. Chem. B 2012, 116, 4206−4211

The transition between a strong osmotic pressure at 0.8e and ion leakage at 0.6e is very sharp, while a more gradual decline in osmotic pressure is observed for strong charges. As the charge becomes stronger, the ion−ion interaction becomes more predominant like in the case of the 2 Å ions: the effective hydrophilicity is increasing albeit this time because of the increase in charge rather than the decrease in radius, and just as was the case with the small 2 Å/1e ions, this leads to a drop in the osmotic pressure induced. Thus, it can be understood that the hydrophilicity of the ions is the defining factor in the effectiveness of the osmosis, and this hydrophilicity is defined through a balance of the ion size and charge. Thus, 1e represents the ideal charge for ions of 4 Å in radius, and it can be expected that smaller ions have a lower optimum charge, while larger ions have a greater optimum charge.

APPLICATION TO REAL-WORLD SOLUTES

Having gained an understanding of how size and charge alter osmosis for the hypothetical ions in this study, one can appreciate the interplay between Na and Cl in real-world solutes and understand how this effects osmosis. For the case of NaCl, upon which this study has its basis, the radii of the Na and Cl ions are 2.583 Å and 4.401 Å, respectively, while they carry opposite charges of magnitude 1e each resulting in an osmotic pressure which is similar in strength to that observed for the medium radii studied here. Using the 4 Å radius ion for comparison, while the hydration of the ions for real NaCl does not differ, the slightly different distribution of the ions in the chamber reveals useful information about the mechanism leading to osmosis for this solute.

Figure 7 shows how the system with real NaCl actually allows a slightly closer approach to the membrane wall than in the 4 Å case. The fact that real Cl approaches most closely to the membrane is expected since its radius is the largest, and it was shown earlier how larger radii approach more closely to the membrane. The closer approach of real Na to the membrane is less expected, and this arises through Na−Cl interaction: because of its small size and enhanced interaction with other atoms, the peak density of real Na around real Cl is 1.6 times higher than that measured for the 4 Å case, and this, coupled with the fact that the density of Na is similar to Cl at all distances, suggests that the Na−Cl coupling is helping Na approach closer to the membrane than it otherwise would do.

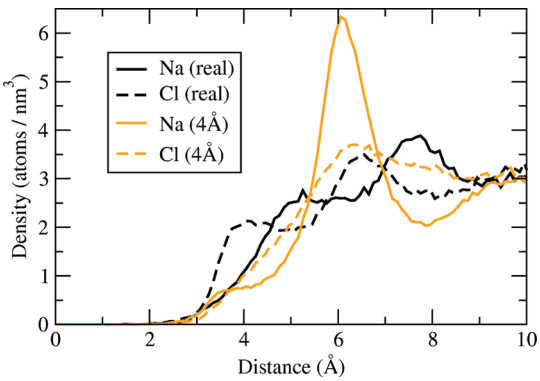

Figure 7. Ion density as a function of distance from the membrane wall for real NaCl and for the 4 Å radius case.

The effect of interion coupling is important for ion transport through nanotubes,[26] and here it can be seen to have a role in osmosis too through its influence on ion position. The peak density of real NaCl is also observed at around 6 Å albeit with a lower peak value. This can be understood to be a consequence of the NaCl coupling leading to an overall smoother distribution of ions. The lower peak density of ions could be expected to reduce the pull on the water, but at the same time, the small Na ion, placed unusually close to the membrane because of coupling with Cl, has an increased influence on water at the membrane. The overall force on the water, therefore, is similar to that of the 4 Å ions, and the net osmotic pressure ultimately remains the same. Thus, through comparison to the hypothetical ions, it is possible to gain an insight into the role of ion size and interaction which lead to the observed osmotic strength of real NaCl.

CONCLUSION

The molecular mechanisms of osmosis and the influence of ion size and charge have been explored with the aim of gaining a clearer understanding of how the choice of solute determines the strength of osmosis.

By utilizing hypothetical ions of various sizes, we have demonstrated that the strongest osmosis occurs for ions of around 3−4 Å radius. This has been shown to arise through their optimal placement relative to water near the membrane wall while maintaining reasonably strong ion−water hydration. This has in turn allowed a greater understanding of the role of interion interaction and positioning in achieving strong osmosis with real NaCl.

Furthermore, by studying the effect of ion charge on osmotic strength, it has been shown that both the charge and the size of the ion are simply mechanisms for defining the ion hydrophilicity, which is ultimately what determines the strength of the osmosis.

Overall, these results demonstrate that the osmotic strength of a solute can be highly sensitive to small changes in size and charge and that careful choice of solute for forward or reverse osmosis applications can significantly enhance the efficiency of such processes.

APPENDIX A: SIZE EFFECTS IN MD

The simulations here make use of a chamber of approximately 45 Å in length. In many simulations which consider ionic phenomena such as osmosis, however, a chamber length of 30 Å is typically used.[16,27,28] In conducting such simulations, it is desirable to use a chamber size which is as small as possible, in order to reduce computational cost, while maintaining a chamber which is large enough to be free of size effects so that the results can be extended to macroscale applications and experiments. To check for any size effects, the osmotic strength of a system with 4 Å ions was checked as a function of the length of the chamber (Figure 8). The results indicate a slightly larger osmotic pressure at 30 Å, while at 45 Å and above the osmotic pressure is consistent to within 1 standard deviation.

Further analysis of the 30 Å and 45 Å cases reveals that while the hydration of the ions and relative positioning of the ions do not change significantly, a slightly denser chamber is required in the case of the 30 Å chamber in order to achieve the same force on the walls measured at 45 Å and above. Therefore, even though the relative positioning of the ions in all chambers is the same, the number of ions per unit z-axis length is slightly higher in the 30 Å case leading to an increase in the net pull of the ions

dx.doi.org/10.1021/jp2113363 | J. Phys. Chem. B 2012, 116, 4206−4211

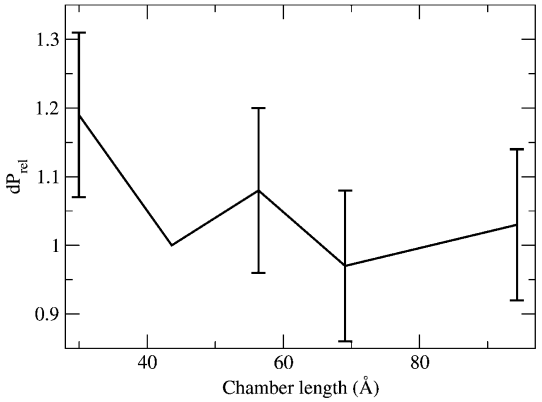

Figure 8. Osmotic pressure as a function of chamber length (SW and PW) for 4 Å radius ions relative to the osmotic pressure measured for the 43.6 Å chamber used in these studies. Cross-axial dimensions are constant at 30 Å each. For a chamber length of 30 Å, the density of the system is notably different from the larger chambers leading to an increase in osmotic pressure. The error bar indicates one standard deviation.

on water and to an increase in the osmotic pressure for the 30 Å chamber.

AUTHOR INFORMATION

Corresponding Author

*E-mail: cannon@photon.t.u-tokyo.ac.jp (J.C.); shiomi@photon.t.u-tokyo.ac.jp (J.S.).

Notes

The authors declare no competing financial interest.

ACKNOWLEDGMENTS

This work is financially supported in part by the Japan Society for the Promotion of Science (JSPS, project 2200064) (J.C. and S.M.), the Mukai Science and Technology Foundation (J.S.), the CFD ERC (NRF 2009-0093136) (D.K.), Grant-in-Aid for Scientific Research (22226006 and 19051016) (J.S. and S.M.), and the Global COE Program Global Center for Excellence for Mechanical Systems Innovation (J.S. and S.M.).

REFERENCES

(1) Lang, F.; Busch, G. L.; Ritter, M.; Volkl, H.; Waldegger, S.; Gulbins, E.; Haussinger, D. *Physiol. Rev.* **1998**, *78*, 247−306.
(2) Dolar, D.; Kosutic, K.; Vucic, B. *Desalination* **2011**, *265*, 237−241.
(3) McCutcheon, J. R.; McGinnis, R. L.; Elimelech, M. *Desalination* **2005**, *174*, 1−11.
(4) Committee on Advancing Desalination Technology, National research council. *Desalination: A national perspective*; The National Academies Press: Washington, DC, 2008.
(5) Kalra, A.; Garde, S.; Hummer, G. *Proc. Natl. Acad. Sci. U.S.A.* **2003**, *100*, 10175−10180.
(6) Majumder, M.; Chopra, N.; Andrews, R.; Hinds, B. J. *Nature* **2005**, *438*, 44−44.
(7) Holt, J. K.; Park, H. G.; Wang, Y. M.; Stadermann, M.; Artyukhin, A. B.; Grigoropoulos, C. P.; Noy, A.; Bakajin, O. *Science* **2006**, *312*, 1034−1037.
(8) Thomas, J. A.; McGaughey, A. J. H. *J. Chem. Phys.* **2008**, *128*, 084715.
(9) Jia, Y. X.; Li, H. L.; Wang, M.; Wu, L. Y.; Hu, Y. D. *Sep. Purif. Technol.* **2010**, *75*, 55−60.
(10) Cannon, J.; Hess, O. *Microfluid. Nanofluid.* **2010**, *8*, 21−31.
(11) Corry, B. *J. Phys. Chem. B* **2008**, *112*, 1427−1434.
(12) Murad, S.; Powles, J. G. *J. Chem. Phys.* **1993**, *99*, 7271−7272.
(13) Kim, K. S.; Davis, I. S.; Macpherson, P. A.; Pedley, T. J.; Hill, A. E. *Proc. Royal Soc. London A* **2005**, *461*, 273−296.
(14) Harder, E.; Walters, D. E.; Bodnar, Y. D.; Faibish, R. S.; Roux, B. *J. Phys. Chem. B* **2009**, *113*, 10177−10182.
(15) Hughes, Z. E.; Gale, J. D. *J. Mater. Chem.* **2010**, *20*, 7788−7799.
(16) Raghunathan, A. V.; Aluru, N. R. *Phys. Rev. Lett.* **2006**, *97*, 024501.
(17) Hockney, R. W.; Eastwood, J. W. *Computer Simulation Using Particles*; Adam Hilger: Bristol, United Kingdom, 1988.
(18) Plimpton, S. *J. Comput. Phys.* **1995**, *117*, 1−19.
(19) Suk, M. E.; Raghunathan, A. V.; Aluru, N. R. *Appl. Phys. Lett.* **2008**, *92*, 133120.
(20) Werder, T.; Walther, J. H.; Jaffe, R. L.; Halicioglu, T.; Koumoutsakos, P. *J. Phys. Chem. B* **2003**, *107*, 1345−1352.
(21) Allen, M. P.; Tildesley, D. *Computer simulation of liquids*; Clarendon: Oxford, United Kingdom, 1987.
(22) Berendsen, H. J. C.; Grigera, J.; Straatsma, T. P. *J. Phys. Chem.* **1987**, *91*, 6269−6271.
(23) Dang, L. X.; Rice, J. E.; Caldwell, J.; Kollman, P. A. *J. Am. Chem. Soc.* **1991**, *113*, 2481−2486.
(24) Dang, L. X.; Kollman, P. A. *J. Phys. Chem.* **1995**, *99*, 55−58.
(25) Callahan, K. M.; Casillas-Ituarte, N. N.; Roeselova, M.; Allen, H. C.; Tobias, D. J. *J. Phys. Chem. A* **2010**, *114*, 5141−5148.
(26) Cannon, J.; Tang, D.; Hur, N.; Kim, D. *J. Phys. Chem. B* **2010**, *114*, 12252−12256.
(27) Raghunathan, A. V.; Aluru, N. R. *Appl. Phys. Lett.* **2006**, *89*, 064107.
(28) Zeng, L.; Zuo, G. H.; Gong, X. J.; Lu, H. J.; Wang, C. L.; Wu, K. F.; Wan, R. Z. *Chin. Phys. Lett.* **2008**, *25*, 1486−1489.